



Chapter 30

Fluorine (^{19}F) MRI for Assessing Inflammatory Cells in the Kidney: Experimental Protocol

Min-Chi Ku, Adrian Schreiber, Paula Ramos Delgado, Philipp Boehm-Sturm, Ralph Kettritz, Thoralf Niendorf, Andreas Pohlmann, and Sonia Waiczies

Abstract

Inflammation is one underlying contributing factor in the pathology of acute and chronic kidney disorders. Phagocytes such as monocytes, neutrophils and dendritic cells are considered to play a deleterious role in the progression of kidney disease but may also contribute to organ homeostasis. The kidney is a target of life-threatening autoimmune disorders such as the antineutrophil cytoplasmic antibody (ANCA)-associated vasculitides (AAV). Neutrophils and monocytes express ANCA antigens and play an important role in the pathogenesis of AAV. Noninvasive in vivo methods that can quantify the distribution of inflammatory cells in the kidney as well as other organs in vivo would be vital to identify the causality and significance of inflammation during disease progression. Here we describe a noninvasive technique to study renal inflammation in rodents in vivo using fluorine (^{19}F) MRI. In this protocol we chose a murine ANCA-AAV model of renal inflammation and made use of nanoparticles prepared from perfluoro-5-crown-15-ether (PFCE) for renal ^{19}F MRI.

This chapter is based upon work from the COST Action PARENCHIMA, a community-driven network funded by the European Cooperation in Science and Technology (COST) program of the European Union, which aims to improve the reproducibility and standardization of renal MRI biomarkers. This experimental protocol chapter is complemented by two separate chapters describing the basic concept and data analysis.

Key words Magnetic resonance imaging (MRI), Fluorine (^{19}F), Nanoparticles (NPs), Inflammation, Kidney, Mice

1 Introduction

Inflammation is one underlying contributing factor in the pathology of acute and chronic kidney disorders [1]. Studies also suggest that systemic inflammation can cause ischemic injury in a vital organ, such as the kidney, which could then result in repercussions in another distant organ downstream of the ischemic event, such as the heart [2–4]. Early inflammatory events governed by cells of the innate immune system, such as macrophages, probably promote

renal tissue injury but may also support repair [5–8]. Phagocytes such as dendritic cells (DC) and macrophages are considered to play a deleterious role in the inflammatory outcome of chronic kidney disease but may also contribute to organ homeostasis [9].

The kidney is often a target of systemic autoimmune disorders that are compounded by complex inflammatory processes [10]. Examples of life-threatening autoimmune disorders that affect the kidneys are the antineutrophil cytoplasmic antibody (ANCA)-associated vasculitides (AAV) manifesting as rapidly progressive necrotizing crescentic glomerulonephritis (NCGN) [11]. Neutrophils and monocytes express ANCA antigens and ANCA induces neutrophil extracellular traps that cause RIPK1-dependent endothelial cell (EC) damage via activation of the alternative complement pathway [12]. While the central role of neutrophil activation in ANCA-associated vasculitis and NCGN is clear, the role of monocytes/macrophages was only recently uncovered in a renal ANCA-associated vasculitis model [13].

Noninvasive *in vivo* methods that can quantify the level of inflammation in the kidney as well as other organs in system autoimmune disorders such as ANCA-associated vasculitides would be vital to identify the causality and significance of inflammation during the course of disease. One method to visualize inflammation by MRI makes use of MR contrast agents that modulate T_2^* and that are easily taken up by phagocytic inflammatory cells [14, 15]. Iron oxide particles including ultrasmall iron oxide agents (USPIO) have been used as susceptibility (T_2^*) MR contrast agents to target inflammatory cell populations. These particles are engulfed by phagocytic cells in the blood. Drawbacks of USPIO-based T_2^* studies include MR signal quantification and difficulty to distinguish contrast created by labeled cells from other intrinsic tissue contrasts [14].

Here we describe an alternative noninvasive technique to study inflammation in rodents *in vivo* using fluorine (^{19}F) MRI. ^{19}F MRI is performed in association with intravenous injections of perfluorocarbon (PFC) nanoparticles (NPs). These NPs are taken up by cells of the immune system traveling through the circulation into the inflammatory regions. Thus ^{19}F MRI is ideal for studying distribution of inflammatory cell *in vivo*. In this protocol we chose a murine AAV model of renal inflammation that has been described in greater depth elsewhere [16] and made use of nanoparticles prepared from perfluoro-5-crown-15-ether (PFCE).

This experimental protocol chapter is complemented by two separate chapters describing the basic concept (please *see* the chapter by Waiczies S et al. “Functional Imaging Using Fluorine (^{19}F) MR Methods: Basic Concepts”) and data analysis (please *see* the chapter by Starke L et al. “Data Preparation Protocol for Low Signal-to-Noise Ratio Fluorine-19 MRI”), which are both part of this book.

This chapter is part of the book Pohlmann A, Niendorf T (eds) (2020) *Preclinical MRI of the Kidney—Methods and Protocols*. Springer, New York.

2 Materials

2.1 Animals

This experimental protocol is tailored for mice with a body mass of 20–30 g (e.g., wild type C57BL/6 mice or a disease model of renal inflammation). Here we describe briefly how to generate the AAV animal model. More thorough detail on the immunization, bone marrow transplantation as well purification of mouse MPO is given in the study establishing the MPO-AAV animal model [16]. Wild-type (WT) C57BL/6J mice (B6) (Jackson Laboratories, Bar Harbor, ME) and myeloperoxidase-deficient (MPO^{-/-}) mice (generated by Aratani et al. [17]) were used in this protocol. MPO^{-/-} mice were immunized with murine MPO at the age of 8–10 weeks, subjected to lethal irradiation, and then transplanted with MPO-expressing bone marrow cells. Animal experiments should be approved by animal welfare authorities and guidelines to minimize discomfort to animals (86/609/EEC).

2.1.1 Lab Equipment

1. NP preparation: Ultrasonic device with ultrasonic power (400 W) and frequency (24 kHz) for stand-mounted operation such as UP400S (Hielscher, Teltow, Germany) to prepare PFCE nanoparticles.
2. NP preparation: Titanium sonotrode for emulsifying samples from 5 to 200 ml (e.g., H3 from Hielscher, Teltow, Germany).
3. NP characterization: Dynamic light scattering instrument such as Zetasizer Nano (Malvern Instruments, Malvern, Worcestershire, UK) to characterize particle size (Z-average) and polydispersity index (PDI) of the PFCE nanoparticles.
4. NP application: Mouse restrainer for intravenous administering the PFCE nanoparticles.
5. Anesthesia: Isoflurane inhalation system which can adjust different levels of isoflurane such as Isoflurane Vapor 19.1 (Draeger, Draegerwerk, Luebeck, Germany). The range of isoflurane level that is used for anesthesia in mice is 0.5–1.5%. Please refer to the chapter by Kaucsar T et al. “Preparation and Monitoring of Small Animals in Renal MRI” for an in-depth description and discussion of the anesthesia.
6. Anesthesia: Mouse chamber connected to isoflurane inhalation system and gas-mixing system to anesthetize mice by inhalation narcosis prior to transfer to the MR scanner.
7. Gases: O₂, and compressed air, as well as a gas-mixing system such as FMI (Föhr Medical Instruments GmbH, Seeheim-Ober Beerbach, Germany) to achieve the required physiological O₂/air mixture in combination with the isoflurane gas.

2.2 MRI Hardware

The general hardware requirements for renal ^1H MRI on mice and rats are described in the chapter by Ramos Delgado P et al. “Hardware Considerations for Preclinical Magnetic Resonance of the Kidney.” The technique described in this chapter was tailored for a 9.4 T MR system (Biospec 94/20, Bruker Biospin, Ettlingen, Germany) but advice for adaptation to other field strengths is given where necessary.

1. $^1\text{H}/^{19}\text{F}$ dual-tunable volume RF coil (35 mm inner diameter, 50 mm length; Rapid Biomed, Würzburg, Germany).
2. $^1\text{H}/^{19}\text{F}$ dual-tunable volume RF coil (18 mm inner diameter, 39 mm length) for ex vivo imaging [18].
3. ^{19}F cryogenic quadrature RF surface probe (^{19}F -CRP) operated at ~ 28 K (*see Note 1*).
4. A physiological monitoring system that can track respiration and temperature during the MR procedure such as the Monitoring & Gating System and PC-sam software from SA Instruments (SAII, Stony Brook, NY, USA).
5. Mouse sled with a breathing mask connected to the isoflurane system.

2.3 MRI Techniques

Typically, ^{19}F MR studies applying PFC compounds such as PFCE to study inflammation in vivo employ the turbo spin echo (SE) rapid acquisition using relaxation enhancement (RARE) sequence [18–22]. This method reduces acquisition time by accumulating multiple echoes within a single repetition time [23]. Typically T_1 of these ^{19}F compounds is in the range of 0.5–3 s, depending on the compound and also magnetic field strength (B_0). However, if employing paramagnetic macrocyclic PFC compounds complexed to lanthanides, T_1 values can be reduced to the order of 1–15 ms and T_2^* values correspondingly reduced to 0.4–12 ms and a radial zero echo time (ZTE) sequence might be better suited [24].

1. ^1H MR sequence: 2D and 3D FLASH protocols are standard sequences on Bruker MRI systems, where they are called “FLASH_2D”, “FLASH_3D” or “1_Localizer_multi_slice” (*see Note 2*).
2. ^{19}F spectroscopy sequence: Block pulse for nonlocalized (global) is a standard sequence on Bruker MRI systems, where it is called “SINGLEPULSE” (*see Note 3*).
3. ^{19}F MR sequence: 3D RARE protocol for measurements. This is a standard sequence on Bruker MRI systems, where it is called “TurboRARE_3D” in Paravision 5, “T2_TurboRARE_3D” in Paravision 6 (*see Note 4*).

3 Methods

3.1 MR Protocol Setup

3.1.1 ¹⁹F MR Imaging

Typically T_1 of PFC compounds is in the range of 0.5–3 s, depending on the compound and also magnetic field strength (B_0). When working with a standard diamagnetic PFC such as PFCE that is documented in the literature, it is recommended that the T_1 and T_2 of the compound be studied at 37 °C before starting with the first in vivo experiments to study inflammation. According to the measured relaxation times (T_1/T_2), the optimal settings for RARE, namely echo train lengths (ETL) and repetition time (TR) should be calculated to improve sensitivity thresholds.

1. *Repetition time (TR)*: for RARE, TR will be limited by ETL and the number of slices. A short TR is desirable for SNR efficiency (0.8–1.5 s depending on T_1) keeping in mind that T_1 will change with changes in oxygenation status (*see Note 5*).
2. *Flip angle (FA)*: for the block pulse and RARE sequence, the FA for the excitation pulse should be at 90°. Additionally the RARE sequence has a refocusing pulse with a FA of 180°. To maximize the SNR and contrast, the flip angle has to be separately calculated for FLASH considering the Ernst angle: $\alpha_E = \cos^{-1}(e^{-TR/T_1})$ which relates FA, T_1 and TR (*see Note 6*).
3. *Echo train length (ETL)*: in RARE, use a value as high as possible to reduce scan time. In the TurboRARE sequence on Bruker MRI systems, ETL is referred to as “rare factor”.
4. *Echo time (TE)*: use the shortest effective TE and echo spacing (ΔTE) possible. Especially for very high ETL, TE can become very long. Centric encoding can be used to reduce the effective TE, generally at the cost of introducing minor image artifacts.
5. *Acquisition bandwidth (BW)*: long enough to shorten the ΔTE without compromising the SNR, which decreases with increasing BW as a result of increased noise level.
6. *Geometry*: Adapt so that whole abdomen fits into FOV in L-R direction (approx. 25 mm for mice) and use frequency encoding in H-F- direction. Choose a 3D volume suited to cover the whole body width and as much of the length of the mouse that the RF coil can afford as possible. With a typical mouse body resonator as the one used in this protocol one could use a FOV of 60 × 30 × 30 mm and matrix size of 400 × 200 × 200 (for ¹H) and 128 × 64 × 64 (for ¹⁹F).
7. *Resolution/acceleration*: Use the highest in-plane resolution that the SNR allows, typically around 100–150 μm for ¹H MR scans and 250–500 μm for ¹⁹F MR scans. Zero-filling in phase encoding direction can be helpful to speed up acquisition while increasing the number of averages to improve SNR

especially for ^{19}F MR scans. One may use half Fourier in read direction (asymmetric echo) to further shorten the first TE. Reducing the excitation pulse length to below 1 ms would then also help to shorten TE.

8. For an example of parameters used in this chapter, please *see* **Notes 7** and **13**.

3.2 ^{19}F Nanoparticle Preparation, Characterization, and Application

1. *NP preparation:* Emulsify 1.2 M PFCE (Fluorochem, Derbyshire, UK) in Pluronic F-68 (Sigma-Aldrich, Germany) for 10 min using a cell disrupting titanium sonotrode connected to an ultrasonic device and employing a continuous pulse program for 60 s. Use ear protection while sonicating the mixture to avoid hearing damage and loss.
2. *NP characterization:* Measure mean particle size (in nm), polydispersity index (PDI), and zeta potential (mV) by using a dynamic light scattering machine such as the one listed above. Use the z-average diameter for particle size since it gives an intensity-weighted harmonic diameter and is ideal for comparing different analyses. The nanoparticles should have a PDI < 0.3 indicating a relatively low polydispersity and narrow size distribution (*see* **Note 8**).
3. *NP application:* Administer ^{19}F nanoparticles via tail vein at a dose of 5–80 μmol of PFCE molecules, depending on the frequency of the bolus injections. Start administering ^{19}F nanoparticles at relevant time-points of your inflammatory model, for example, in MPO immunized MPO $^{-/-}$ mice subjected to lethal irradiation we started intravenous application of PFCE nanoparticles 4–8 weeks following transplantation of MPO-expressing bone marrow cells (*see* **Note 9**).

3.3 Preparation Prior to $^{19}\text{F}/^1\text{H}$ MRI Scans

Four to 18 h following the last intravenous administration of ^{19}F nanoparticles prepare the mice for $^{19}\text{F}/^1\text{H}$ MRI:

1. First anesthetize the mice by inhalation narcosis using a mouse chamber connected to a isoflurane inhalation system and gas-mixing system (*see* **Note 10**).
2. Adjust the flow rate for air and O_2 at 0.2 and 0.1 l/min respectively and 3% isoflurane (adjusted from a vaporizer) for about 2 min until the required level of anesthesia is reached (no response following toe pinch).
3. Transfer mice to the MR scanner. Should a quantification of inflammation be required, a reference tube with a known concentration of ^{19}F nanoparticles should be placed in proximity to the region of interest. For quantification of signal please refer to the chapter by Starke L et al. “Data Preparation Protocol for Low Signal-to-Noise Ratio Fluorine-19 MRI.”

4. While keeping the flow rate for air and O₂ constant, adjust the isoflurane vaporizer to 0.8–1.5% until an optimal breathing pattern is reached.
5. Set up the temperature monitoring (rectal probe) and respiratory monitoring (balloon on chest) unit. A respiratory rate of 70–90 breaths per minute is recommended. Keep the body temperature at 36–37 °C during the experiment by employing a warm water (or alternatively warm air) circulation system.
6. Tune the RF coil to both the ¹H resonance frequency (e.g., 400.1 MHz for 9.4 T) and to the ¹⁹F resonance frequency (e.g., 376.3 MHz for 9.4 T) and match the characteristic impedance of the coil to 50 Ω using the tuning monitor of the animal MR scanner.
7. Perform anatomical imaging as described in the chapter by Pohlmann A et al. “Essential Practical Steps for MRI of the Kidney in Experimental Research.” Set up a 2D FLASH protocol for the acquisition of anatomical kidney ¹H scans (*see Note 7*).
8. Perform localized shimming on the kidney imaging as described in the chapter by Pohlmann A et al. “Essential Practical Steps for MRI of the Kidney in Experimental Research” (*see Note 11*).
9. Save the parameters of all adjustments (such as iterative shimming calculations and reference power values) performed during the first ¹H scans for application into the ¹⁹F scans.

3.4 ¹⁹F/¹H MRI of the Kidney

3.4.1 *In Vivo* ¹⁹F/¹H MRI Using a Room Temperature Mouse Body Volume ¹⁹F/¹H RF Resonator

Following acquisition of the anatomical ¹H kidney scans, *in vivo* ¹⁹F MR images of the kidney can be acquired and later overlaid onto the ¹H MR images. An example of an *in vivo* ¹H/¹⁹F MRI is shown in Fig. 1.

1. Load the SINGLEPULSE FID-sequence with a TR of at least 1000 ms.
2. Set nucleus to ¹⁹F (e.g., in “Open Edit Scan” in Bruker’s Paravision 5.1 or “System” tab in Bruker’s Paravision 6). Since the ¹⁹F MR signal is too low for automatic adjustments, apply the same settings used for the ¹H anatomical scans (*see Note 12*).
3. Deselect the automatic reference gain (RG) and set on maximum (e.g., in Edit Method in Bruker’s Paravision 5.1 or using the “Instruction” tab (GOP) and “Setup” tab in Paravision 6).
4. Start the SINGLEPULSE sequence using setup mode. If the ¹⁹F spectral signal within the acquisition-window is too low, add more averages until a signal is clearly visible. Adjust the basic frequency in order to center the ¹⁹F spectral peak at 0 Hz in the acquisition window. Apply this basic frequency, press Stop and apply.

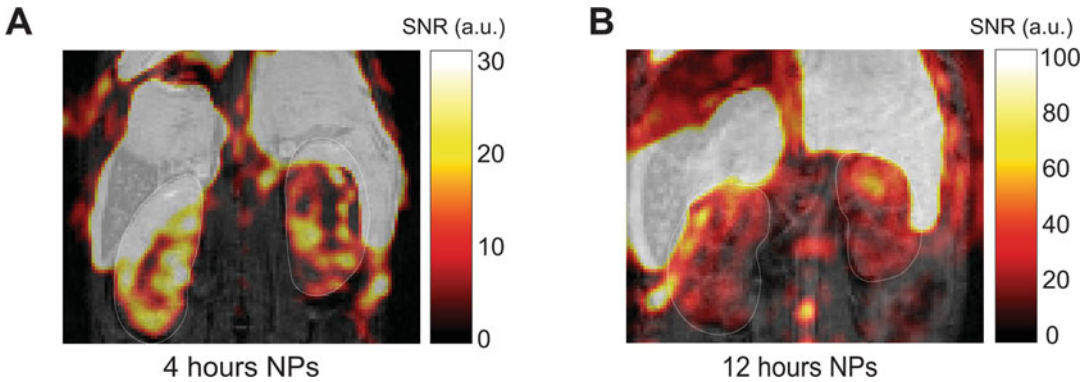


Fig. 1 In vivo $^{19}\text{F}/^1\text{H}$ MRI of a murine ANCA-AAV model of renal inflammation using the $^1\text{H}/^{19}\text{F}$ dual-tunable volume RF coil (35 mm inner diameter). Eight weeks following transplantation of bone marrow cells, MPO-AAV mice were administered one bolus of PFCE nanoparticles (NPs) intravenously (80 μmol in 100 μl) and $^{19}\text{F}/^1\text{H}$ MRI was performed 4 h (a) and 12 h (b) thereafter. (1) ^1H 2D FLASH protocol: TR = 579.4 ms, TE = 5 ms, FA = 75, matrix = 256×128 . (2) ^{19}F 3D RARE protocol: TR = 800 ms, TE = 6.16 ms, Matrix = $256 \times 128 \times 128$, RARE Factor = 32

5. Setup a TurboRARE 3D protocol for the ^{19}F scans.
6. Use the same geometry used for anatomical ^1H imaging but reduce the matrix size for increased SNR and use a rare factor of at least 32. Set nucleus to ^{19}F . Deselect automatic adjustments (as above). For an example of parameters, please *see* **Note 7**.
7. When the scans are finished retract the mouse-holder from the MR scanner. Disconnect the mouse carefully from the holder. If the mouse is not sacrificed for ex vivo analysis (e.g., high resolution ^{19}F MRI of the kidney, see below) following the MR scans, closely monitor until it has completely recovered from anesthesia. Body temperature regulation might still be affected after the anesthesia, so during the recovery process, put the mouse in a separate cage that is placed on a warm temperature regulated pad. Once the mouse has completely recovered from anesthesia, you may return it to its holding cage and to the animal room.

3.4.2 High Spatial Resolution ^{19}F MRI of Ex Vivo Kidney Using a ^{19}F CryoProbe

Kidney inflammation can also be studied with high spatial resolution ex vivo ^{19}F MRI, for example, by using a transceive ^{19}F CryoProbe, which we previously used to study brain inflammation in a model of CNS autoimmunity [25]. An example of a high resolved ex vivo $^1\text{H}/^{19}\text{F}$ MRI of the kidney is shown in Fig. 2.

1. At the end of the in vivo experiment, anesthetize mice with a terminal dose of ketamine and xylazine. Ensure the required level of anesthesia is reached (no response following toe pinch).
2. Transcardially perfuse mouse with 20 ml PBS followed by 20 ml 4% paraformaldehyde.

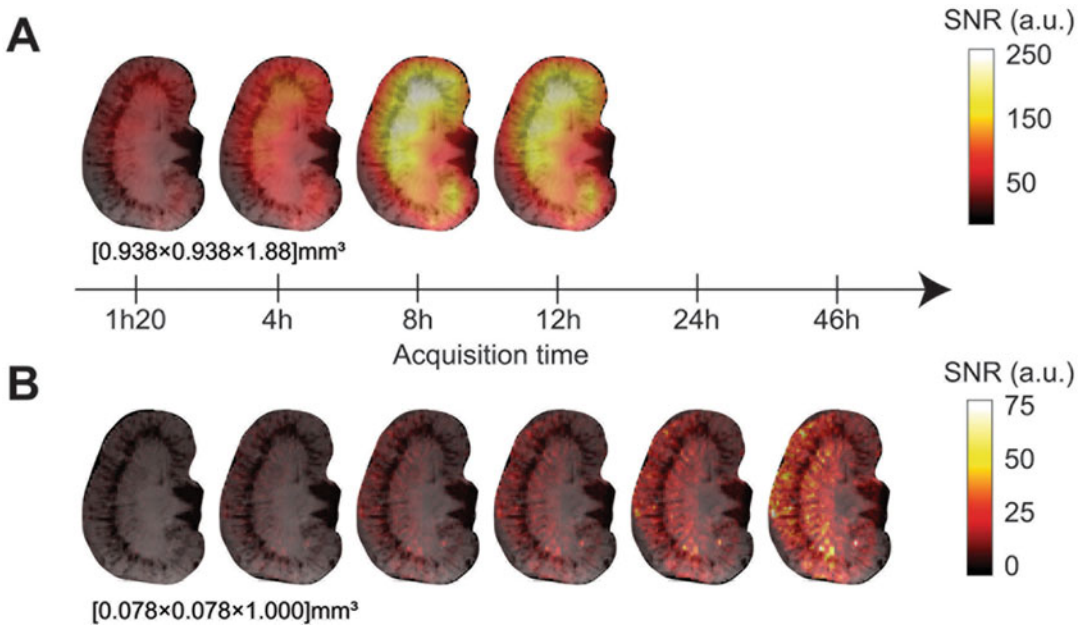


Fig. 2 Ex vivo $^{19}\text{F}/^1\text{H}$ MRI of an inflamed kidney from the ANCA-AAV model. (a) Low spatial resolution images acquired using the $^1\text{H}/^{19}\text{F}$ dual-tunable volume RF coil (18 mm inner diameter). At this resolution $[0.938 \times 0.938] \text{mm}^2$, a high ^{19}F signal can be achieved already after 1 h acquisition time. However, anatomical detail is lacking in the ^{19}F MR images. (b) High spatial resolution images acquired with the ^{19}F cryogenic quadrature RF surface probe (^{19}F -CRP). The gain in SNR achieved by the ^{19}F -CRP was used to increase the in plane spatial resolution $[0.078 \times 0.078] \text{mm}^2$

3. Harvest relevant organs (e.g., kidney, liver, and spleen).
4. Transfer organs to a container filled with 4% PFA and store at 4°C .
5. Prior to the high resolution ^{19}F MRI of the kidney, embed the kidney in 1% low melting agarose in a 1.5 ml Eppendorf tube.
6. ^{19}F -CRP adjustments: since the ^{19}F signal is too low for automatic adjustments, use a ^{19}F calibration phantom (fill highly fluorinated substance such as trifluoroethanol with water in a 1.5 ml Eppendorf tube. Place the ^{19}F calibration tube under the ^{19}F -CRP and repeat steps 13–16 to calculate the working frequency. Load and run a `1_Localizer_multi_slice` sequence (see above). Adjust the reference power using the adjustments platform: select a coronal slice of 2 mm thickness and place it close to the RF coil's surface. Select an initial power two orders of magnitude smaller than what is usually expected and press start. Run the rest of the adjustments using the same sequence. Save the shim settings.
7. ^{19}F -CRP imaging: place the ex vivo kidney embedded in a 1.5 ml Eppendorf tube under the ^{19}F -CRP surface. Run the working frequency adjustments as per 13–16, load the shim

calculations, and adjust the reference power as described above. Set the RG to maximum. Load a 2D FLASH protocol and set it up for ^{19}F imaging. Examples for high and medium resolution ^{19}F imaging are given in **Note 13**.

8. Set up a 2D FLASH protocol for the acquisition of anatomical kidney ^1H scans. Use the same geometry used for ^{19}F imaging (*see* **Note 13**).

4 Notes

1. The transceive ^{19}F cryogenic quadrature RF surface probe (^{19}F CryoProbe) operates at ~ 28 K with a dual cooled preamplifier at the base running at ~ 77 K. It has a similar geometry to the existing Bruker ^1H quadrature CryoProbes. More details on the ^{19}F CryoProbe are available in our previous study [25].
2. The FLASH_3D protocol is especially adapted for whole-body imaging of mice (the gradient-system and the volume-resonator need to have a linear region of about 8 cm).
3. The block pulse program (SINGLEPULSE) contains the necessary elements for a simple transmit/receive experiment, sending a pulse and acquiring an FID afterward.
4. A 2D version of this sequence is also available, which allows thicker slices for a general overview but suffers from low SNR for most in vivo applications.
5. Special attention should be given when studying inflammation in models where tissue oxygen levels are likely to change, for example, following ischemic events. In these cases, T_1 weighting needs to be reduced at cost of SNR efficiency by increasing $\text{TR} \gg T_1$ (typically $\text{TR} = 3\text{--}5 \times T_1$).
6. When using transmit-receive surface coils a B_1 correction should be considered in order to compensate for the intrinsic spatial gradient in coil sensitivity (B_1^-) and excitation field (B_1^+ inhomogeneity), which results in significant variation in the excitation FA, decreasing with increasing distance from the RF coil surface. This severely reduces image homogeneity and hampers the acquisition of the absolute signal intensity values for ^{19}F quantification techniques.
7. Example for a 30 g mouse at 9.4 T and FOV of $50 \times 25 \times 25$ mm, (1) ^1H 2D FLASH protocol: $\text{TR} = 579.4$ ms, $\text{TE} = 5$ ms, $\text{FA} = 75$, matrix = 256×128 . (2) ^{19}F 3D RARE protocol: $\text{TR} = 800$ ms, $\text{TE} = 6.16$ ms, Matrix = $256 \times 128 \times 128$, RARE Factor = 32–64.

8. The polydispersity index (PdI) is extrapolated from the DLS function and quantitatively describes the particle size distribution best. PdI ranges from 0.01 for monodispersed particles to 0.7 for particles that have a very broad size distribution. The z-average diameter gives the mean diameter based on intensity of scattered light and sensitive to presence of large particles, peak diameter, peak width, and PdI.
9. In MPO-AAV mice we administered one bolus of PFCE nanoparticles intravenously (80 μmol in 100 μl) 8 weeks following transplantation of bone marrow cells.
10. Mice can be alternatively anesthetized with an intraperitoneal injection of ketamine and xylazine.
11. Shimming is particularly important, since macroscopic magnetic field inhomogeneities affect the exact resonance frequency of the PFCE compounds and might affect quantification of the ¹⁹F MR signal. Shimming should be performed on a voxel enclosing both kidneys using either the default iterative shimming method or the Mapshim technique (recommended). However, the Mapshim technique is not available for X-nuclei-only RF coils. An alternative in this case is to use a highly fluorinated sample to calculate the shims.
12. Since the NMR properties of ¹⁹F and ¹H are similar, the same MR setup and MR parameter settings can be used for both nuclei.
13. Example for ex vivo *high-resolved* ¹⁹F MRI at 9.4 T using the ¹⁹F-CRP and a 2D FLASH: TR = 11 ms, TE = 2.7 ms, FA = 30, Avg = 2250, Repetitions = 35, FOV = 20 × 20, matrix = 256 × 256, 1 mm slice thickness. Example for ex vivo *low-resolved* ¹⁹F MRI at 9.4 T using the ¹H/¹⁹F dual-tunable volume RF coil (18 mm inner diameter) and a 3D RARE method: TR = 800 ms, TE = 5 ms, Avg = 256, Repetitions = 13, FOV = 60 × 30 × 30, matrix = 64 × 32 × 16. ¹H 2D FLASH protocol: TR = 18.7 ms, TE = 5.5 ms, FA = 25, matrix = 171 × 256, 1 mm slice thickness.

Acknowledgments

This work was funded, in part (Adrian Schreiber, Ralph Kettritz, Thoralf Niendorf, Sonia Waiczies, and Andreas Pohlmann), by the German Research Foundation (Gefördert durch die Deutsche Forschungsgemeinschaft (DFG), Projektnummer 394046635, SFB 1365, RENOPROTECTION. Funded by the Deutsche Forschungsgemeinschaft (DFG, German Research Foundation), Project number 394046635, SFB 1365, RENOPROTECTION).

Also, our research is funded by the Deutsche Forschungsgemeinschaft to SW (DFG WA2804), AP (DFG PO1869), and AS (DFG SCHR7718).

This chapter is based upon work from COST Action PARENCH IMA, supported by European Cooperation in Science and Technology (COST). COST (www.cost.eu) is a funding agency for research and innovation networks. COST Actions help connect research initiatives across Europe and enable scientists to enrich their ideas by sharing them with their peers. This boosts their research, career, and innovation.

PARENCHIMA (renalmri.org) is a community-driven Action in the COST program of the European Union, which unites more than 200 experts in renal MRI from 30 countries with the aim to improve the reproducibility and standardization of renal MRI biomarkers.

References

- Chawla LS, Eggers PW, Star RA, Kimmel PL (2014) Acute kidney injury and chronic kidney disease as interconnected syndromes. *N Engl J Med* 371(1):58–66. <https://doi.org/10.1056/NEJMr1214243>
- Levy EM, Viscoli CM, Horwitz RI (1996) The effect of acute renal failure on mortality. a cohort analysis. *JAMA* 275(19):1489–1494
- Jorres A, Gahl GM, Dobis C, Polenakovic MH, Cakalaroski K, Rutkowski B, Kisielnicka E, Krieter DH, Rumpf KW, Guenther C, Gaus W, Hoegel J (1999) Haemodialysis-membrane biocompatibility and mortality of patients with dialysis-dependent acute renal failure: a prospective randomised multicentre trial. International Multicentre Study Group. *Lancet* 354(9187):1337–1341
- Brouns R, De Deyn PP (2004) Neurological complications in renal failure: a review. *Clin Neurol Neurosurg* 107(1):1–16. <https://doi.org/10.1016/j.clineuro.2004.07.012>
- Chawla LS, Bellomo R, Bihorac A, Goldstein SL, Siew ED, Bagshaw SM, Bittleman D, Cruz D, Endre Z, Fitzgerald RL, Forni L, Kane-Gill SL, Hoste E, Koyner J, Liu KD, Macedo E, Mehta R, Murray P, Nadim M, Ostermann M, Palevsky PM, Pannu N, Rosner M, Wald R, Zarbock A, Ronco C, Kellum JA (2017) Acute kidney disease and renal recovery: consensus report of the Acute Disease Quality Initiative (ADQI) 16 Workgroup. *Nat Rev Nephrol* 13(4):241–257
- Humphreys BD, Cantaluppi V, Portilla D, Singbartl K, Yang L, Rosner MH, Kellum JA, Ronco C (2016) Targeting endogenous repair pathways after AKI. *J Am Soc Nephrol* 27(4):990–998
- Kurts C, Panzer U, Anders H-J, Rees AJ (2013) The immune system and kidney disease: basic concepts and clinical implications. *Nat Rev Immunol* 13:738. <https://doi.org/10.1038/nri3523>. <https://www.nature.com/articles/nri3523-supplementary-information>
- Bellomo R, Kellum JA, Ronco C, Wald R, Martensson J, Maiden M, Bagshaw SM, Glassford NJ, Lankadeva Y, Vaara ST, Schneider A (2017) Acute kidney injury in sepsis. *Intensive Care Med* 43(6):816–828
- Weisheit CK, Engel DR, Kurts C (2015) Dendritic cells and macrophages: sentinels in the kidney. *Clin J Am Soc Nephrol* 10(10):1841–1851. <https://doi.org/10.2215/cjn.07100714>
- Kurts C, Panzer U, Anders H-J, Rees AJ (2013) The immune system and kidney disease: basic concepts and clinical implications. *Nat Rev Immunol* 13:738. <https://doi.org/10.1038/nri3523>. <https://www.nature.com/articles/nri3523-supplementary-information>
- Furuta S, Jayne DRW (2013) Antineutrophil cytoplasm antibody-associated vasculitis: recent developments. *Kidney Int* 84(2):244–249. <https://doi.org/10.1038/ki.2013.24>
- Schreiber A, Rousselle A, Becker JU, von Mässenhausen A, Linkermann A, Kettritz R (2017) Necroptosis controls NET generation and mediates complement activation, endothelial damage, and autoimmune vasculitis. *Proc Natl Acad Sci* 114(45):E9618–E9625. <https://doi.org/10.1073/pnas.1708247114>

13. Rousselle A, Kettritz R, Schreiber A (2017) Monocytes promote crescent formation in anti-myeloperoxidase antibody-induced glomerulonephritis. *Am J Pathol* 187(9):1908–1915. <https://doi.org/10.1016/j.ajpath.2017.05.003>
14. Grenier N, Merville P, Combe C (2016) Radiologic imaging of the renal parenchyma structure and function. *Nat Rev Nephrol* 12(6):348–359
15. Hueper K, Gutberlet M, Bräsen JH, Jang M-S, Thorenz A, Chen R, Hertel B, Barrmeyer A, Schmidbauer M, Meier M, von Vietinghoff S, Khalifa A, Hartung D, Haller H, Wacker F, Rong S, Gueler F (2016) Multiparametric functional MRI: non-invasive imaging of inflammation and edema formation after kidney transplantation in mice. *PLoS One* 11(9):e0162705. <https://doi.org/10.1371/journal.pone.0162705>
16. Schreiber A, Xiao H, Falk RJ, Jennette JC (2006) Bone marrow-derived cells are sufficient and necessary targets to mediate glomerulonephritis and vasculitis induced by anti-myeloperoxidase antibodies. *J Am Soc Nephrol* 17(12):3355–3364. <https://doi.org/10.1681/asn.2006070718>
17. Aratani Y, Koyama H, Nyui S, Suzuki K, Kura F, Maeda N (1999) Severe impairment in early host defense against *Candida albicans* in mice deficient in myeloperoxidase. *Infect Immun* 67(4):1828–1836
18. Waiczies H, Lepore S, Drechsler S, Qadri F, Purfürst B, Sydow K, Dathe M, Kuhne A, Lindel T, Hoffmann W, Pohlmann A, Niendorf T, Waiczies S (2013) Visualizing brain inflammation with a shingled-leg radiofrequency head probe for 19F/1H MRI. *Sci Rep* 3:1280. <https://doi.org/10.1038/srep01280>
19. Srinivas M, Morel PA, Ernst LA, Laidlaw DH, Ahrens ET (2007) Fluorine-19 MRI for visualization and quantification of cell migration in a diabetes model. *Magn Reson Med* 58(4):725–734. <https://doi.org/10.1002/mrm.21352>
20. Flögel U, Ding Z, Hardung H, Jander S, Reichmann G, Jacoby C, Schubert R, Schrader J (2008) In vivo monitoring of inflammation after cardiac and cerebral ischemia by fluorine magnetic resonance imaging. *Circulation* 118(2):140–148
21. Jacoby C, Temme S, Mayenfels F, Benoit N, Krafft MP, Schubert R, Schrader J, Flögel U (2014) Probing different perfluorocarbons for in vivo inflammation imaging by 19F MRI: image reconstruction, biological half-lives and sensitivity. *NMR Biomed* 27(3):261–271. <https://doi.org/10.1002/nbm.3059>
22. Flögel U, Burghoff S, van Lent PL, Temme S, Galbarz L, Ding Z, El-Tayeb A, Huels S, Bonner F, Borg N, Jacoby C, Muller CE, van den Berg WB, Schrader J (2012) Selective activation of adenosine A2A receptors on immune cells by a CD73-dependent prodrug suppresses joint inflammation in experimental rheumatoid arthritis. *Sci Transl Med* 4(146):146ra108. <https://doi.org/10.1126/scitranslmed.3003717>
23. Hennig J, Nauwerth A, Friedburg H (1986) RARE imaging: a fast imaging method for clinical MR. *Magn Reson Med* 3:823–833. <https://doi.org/10.1002/mrm.1910030602>
24. Schmid F, Hölte C, Parker D, Faber C (2013) Boosting 19F MRI—SNR efficient detection of paramagnetic contrast agents using ultrafast sequences. *Magn Reson Med* 69(4):1056–1062. <https://doi.org/10.1002/mrm.24341>
25. Waiczies S, Millward JM, Starke L, Delgado PR, Huelnhagen T, Prinz C, Marek D, Wecker D, Wissmann R, Koch SP, Boehm-Sturm P, Waiczies H, Niendorf T, Pohlmann A (2017) Enhanced fluorine-19 MRI sensitivity using a cryogenic radiofrequency probe: technical developments and ex vivo demonstration in a mouse model of neuroinflammation. *Sci Rep* 7(1):9808. <https://doi.org/10.1038/s41598-017-09622-2>

Open Access This chapter is licensed under the terms of the Creative Commons Attribution 4.0 International License (<http://creativecommons.org/licenses/by/4.0/>), which permits use, sharing, adaptation, distribution and reproduction in any medium or format, as long as you give appropriate credit to the original author(s) and the source, provide a link to the Creative Commons license and indicate if changes were made.

The images or other third party material in this chapter are included in the chapter's Creative Commons license, unless indicated otherwise in a credit line to the material. If material is not included in the chapter's Creative Commons license and your intended use is not permitted by statutory regulation or exceeds the permitted use, you will need to obtain permission directly from the copyright holder.

